PROTEINS: Structure, Function, and Genetics 44:63–72 (2001)

Proline-Induced Hinges in Transmembrane Helices: Possible Roles in Ion Channel Gating

D. Peter Tieleman, Indira H. Shrivastava, Martin R. Ulmschneider, and Mark S.P. Sansom*
Laboratory of Molecular Biophysics, Department of Biochemistry, University of Oxford, Oxford, United Kingdom

ABSTRACT **A number of ion channels contain transmembrane (TM) α-helices that contain proline-induced molecular hinges. These TM helices include the channel-forming peptide alamethicin (Alm), the S6 helix from voltage-gated potassium (Kv) channels, and the D5 helix from voltage-gated chloride (CLC) channels. For both Alm and KvS6, experimental data implicate hinge-bending motions of the helix in an aspect of channel gating. We have compared the hinge-bending motions of these TM helices in bilayer-like environments by multi-nanosecond MD simulations in an attempt to describe motions of these helices that may underlie possible modes of channel gating. Alm is an α-helical channel-forming peptide, which contains a central kink associated with a Gly-x-x-Pro motif in its sequence. Simulations of Alm in a TM orientation for 10 ns in an octane slab indicate that the Gly-x-x-Pro motif acts as a molecular hinge. The S6 helix from Shaker Kv channels contains a Pro-Val-Pro motif. Modeling studies and recent experimental data suggest that the KvS6 helix may be kinked in the vicinity of this motif. Simulations (10 ns) of an isolated KvS6 helix in an octane slab and in a POPC bilayer reveal hinge-bending motions. A pattern-matching approach was used to search for possible hinge-bending motifs in the TM helices of other ion channel proteins. This uncovered a conserved Gly-x-Pro motif in TM helix D5 of CLC channels. MD simulations of a model of hCLC1-D5 spanning an octane slab suggest that this channel also contains a TM helix that undergoes hinge-bending motion. In conclusion, our simulations suggest a model in which hinge-bending motions of TM helices may play a functional role in the gating mechanisms of several different families of ion channels. Proteins 2001;44:63–72.** © 2001 Wiley-Liss, Inc.

INTRODUCTION

Transmembrane signaling by ion channels couples a signal (e.g., a change in transmembrane voltage) to a response (opening of the channel resulting in flow of ions across a cell membrane). This process is referred to as "gating." Structurally, ion channel proteins have a bilayer-spanning domain architecture based on transmembrane (TM) α-helices, as seen in X-ray structures of two bacterial ion channels.[1,2] Gating must involve conformational changes in the channel protein. Such conformational changes may, in addition to rigid body rearrangements of helix packing,[3] involve intra-helical conformational transitions. Proline-containing sequence motifs in such helices have emerged as key elements in possible conformational "switches" underlying gating of some channels.[4]

There is a considerable literature documenting the frequent presence of proline residues in TM α-helices,[5] even though proline is uncommon within α-helices of water-soluble proteins.[6] Early investigations of structural roles of prolines in integral membrane proteins[7,8] suggested they might play an important role in TM helix bundle architecture. More recent bioinformatics approaches have established the statistical significance of the occurrence of proline-containing motifs in TM α-helices.[9]

There is some evidence suggesting that proline-containing α-helices may play an important role in ion channels,[10,11] especially in the context of voltage-dependent channel gating.[12] Proline residues are seen in the TM α-helices formed by the model voltage-gated channel-forming peptide alamethicin,[13] in the related peptide melittin,[14] and in the sixth TM α-helix of voltage-gated potassium (Kv) channels.[15] It, thus, seems worthwhile to investigate the conformational dynamics of ion channel TM α-helices containing a proline residue when in a bilayer environment in somewhat more detail than has been done previously.

One way in which such conformational dynamics may be investigated is via simulation studies. Earlier investigations used simulations in vacuo to examine the conformational dynamics of intra-helical prolines.[15–20] However, improvements in simulation methodology and in computer performance have enabled simulations of TM α-helices and integral membrane proteins in either a fully solvated lipid bilayer or in an alkane slab.[21,22] The latter provides a mimic of a bilayer environment in which greater helix movement is possible as motions of alkane molecules in the membrane plane are several orders of magnitude faster than those of lipid molecules.

Grant sponsor: The Wellcome Trust.

D. Peter Tieleman's present address is Department of Biological Sciences, University of Calgary, 2500 University Drive NW, Calgary, Alberta, Canada T2N 1N4.

*Correspondence to: Mark S.P. Sansom, Laboratory of Molecular Biophysics, Department of Biochemistry, University of Oxford, South Parks Road, Oxford, OX1 3QU, UK. E-mail: mark@biop.ox.ac.uk

Received 22 August 2000; Accepted 22 March 2001

In this article, we explore the conformational dynamics of a number of proline-containing α-helices from voltage-gated ion channels. The majority of simulations use an octane slab as a bilayer mimetic environment, although a simulation in a phospholipid membrane (an extension of a previous shorter simulation[23]) is included for the purposes of comparison. We show that a number of proline-containing sequence motifs can introduce a dynamic hinge into a TM helix and discuss how such hinges may play a role in voltage gating and/or helix insertion into a bilayer.

METHODS

Setup of the Simulation Systems

Modelling of TM α-helices

Initial models of helices were generated via restrained MD simulations in vacuo, using the simulated annealing protocol described in previous papers.[15,24] For those helices (S6, D6) that form parts of larger proteins, multiple TM helix prediction methods were used, namely: TopPred2 (http://bioweb.pasteur.fr/seqanal/interfaces/toppred.html;[25]); TMAP (http://www.mbb.ki.se/tmap/index.html;[26,27]); DAS (http://www.sbc.su.se/~miklos/DAS/;[28]); PHDhtm (http://www.embl-heidelberg.de/predictprotein/predictprotein.html;[29,30]); memsat (http://globin.bio.warwick.ac.uk/~jones/memsat.html;[31]); TMHMM(http://www.cbs.dtu.dk/services/TMHMM-1.0/;[32]); and TMPred (http://www.ch.embnet.org/software/TMPRED_form.html;[33]), in order to arrive at a consensus length for the TM helix.

Peptide/octane systems

Pre-equilibrated water and octane systems were made at 300 K with a lateral size of 4 × 4 nm. The two systems were merged and simulated for a nanosecond with constant x and y box dimensions, while the pressure was allowed to fluctuate in the z dimension. A system with a peptide helix spanning the resultant octane "membrane" was generated as described in Tieleman et al.[34]. This setup was used for the Alm, Ala20, and hCLC1-D5 simulations. For the KvS6 simulations, a somewhat different setup was employed (see *KvS6 simulations* below) in order to facilitate comparison with the POPC simulations.

For the Alm-octane and related simulations, we used the GROMOS96 43a2 force field as implemented in GROMACS.[35] The water model used was SPC.[36,37] A twin-range cutoff of 0.8/1.4 nm for both Coulomb and Lennard Jones interactions was used. The time step was 5 fs, using hydrogen atoms with an increased mass of 4 amu and a special treatment of hydrogens and aromatic rings.[38] This approach has been used in previous simulations of Alm/octane systems.[34] Briefly, this method entails calculating the forces on the hydrogens, but instead of updating the positions of the hydrogens with these forces, the forces are redistributed over neighboring heavy atoms, and the position of the hydrogen is reconstructed every step assuming an ideal geometry. This effectively removes the degrees of freedom involving the hydrogen atoms while still generating correct forces and pressure for the system as a whole. For the positions of the carbons in an aromatic ring, which is a construct of improper dihedrals, a similar method is used. The neighbor list was updated every 3 steps. Bond lengths were constrained with LINCS.[39] Water, protein, and octane were coupled separately to a temperature bath at 300 K with $\tau_T = 0.1$ ps. The surface area of the system was fixed, but the pressure in the z direction was kept at 1 bar using weak pressure coupling, with $\tau_P = 1.0$ ps.[40]

KvS6 simulations

MD simulations of a KvS6 helix spanning a POPC bilayer were set up and run as described in a previous article.[23] KvS6 simulations in octane used essentially the same conditions (but with a constant box size in *xy*; see above).

Analysis of Results

General

All simulations and analyses were done using the GROMACS suite of programs. Molecular graphics images were generated using Molscript[41] and Raster3D.[42] Helix kink angles were calculated as the angle between the line joining the average Cα position of the first 4 N-terminal residues and the average Cα position of the last 3 residues before a pivot residue and the line joining the average coordinates of the 4 Cα atoms after the pivot and the average position of 3 Cα atoms at the C-terminus. The calculated kink angles were checked to be fairly insensitive to the choice of pivot residue (typically just before the proline hinge). Percentage helicity was calculated as a time average per residue, based on backbone torsion (ϕ,ψ) angles and H-bonding patterns.

Essential dynamics and DynDom

Domain motion was analyzed by a combination of essential dynamics[43,44] and the rigid body domain analysis program DynDom.[44,45] Essential dynamics analysis extracts cooperative motions from a protein dynamics trajectory.[43] It yields a set of eigenvectors, sorted by eigenvalue, which describe collective coordinates in which the main motion occurs. Each of the three collective modes of motion with the highest amplitude is analyzed to find the two structures that differ most from each other. These extremes provide an idea of the nature of the collective mode. They also serve as input structures for the domain analysis program DynDom, which takes two different structures of a protein, and analyzes the difference between the two structures in terms of rigid body motion of domains within the structure. This generates an assignment of domains in the protein, and an analysis of the relative motion between these domains. If domains are found, DynDom calculates a screw axis and an angle of rotation around this axis for one domain with respect to the other. Depending on the direction of this screw axis, motion is classified as twist (screw axis parallel to the axis between the center of mass of two domains) or closure (screw axis perpendicular to the axis between the center of mass of two domains), or something in between. In the latter case, a percentage closure motion is given, which is calculated from the projection of the screw axis on a line perpendicular to the axis between the center of mass of two domains. If the

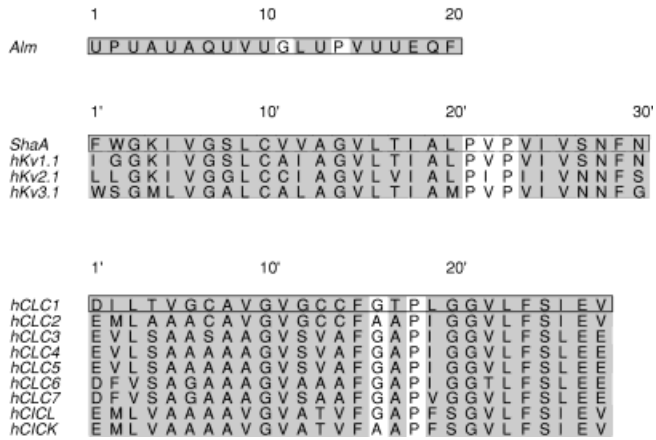

Fig. 1. Sequence of the helices simulated, comparing Alm (note: U = Aib), K channel S6, and chloride channel D5 sequences. The Alm sequence is shown without the N-terminal acetyl group and the C-terminal alcohol that replaces the carboxyl group. The white boxes highlight the GxxP motif. In the sequence alignment of predicted S6 helix sequences, four Kv sequences are shown. The white band indicates the conserved P-[V,I]-P motif. The boxed sequence (ShaA) is that used in the simulations. In the sequence alignment of predicted human CLC D5 helix sequences, the white band indicates the conserved GxP motif. The boxed sequence (hCLC1) is that used in the simulations.

screw axis passes sufficiently close to residues, those residues are said to form a mechanical hinge.

RESULTS

Alm vs. Ala_{20}

Our first simulations are of the antimicrobial peptide alamethicin (Alm).[13,46,47] As can be seen from the sequence (Fig. 1), this contains a central GxxP motif. X-ray[48] and NMR[49] studies indicate that this introduces a kink into the α-helical backbone of Alm. More recent NMR[50] and simulation[51] studies have indicated that this kink may act as a dynamic hinge. However, the time scale of the simulations was relatively short. In order to explore the hinge bending dynamics of Alm more thoroughly, we ran a 10-ns MD simulation of Alm embedded in an octane slab (Table I). As can be seen from Figure 2(A), the initial Alm helix model was oriented so as to the span the octane slab, the latter thus providing a mimic of the hydrocarbon core of a lipid bilayer. For the purposes of comparison, a similar simulation was run for an N- and C-terminally capped Ala_{20} helix, thus providing a simple model of a hydrophobic helix without a proline residue.

The dynamics of a TM-helix based hinge may be considered in terms of two sorts of motion: (1) hinge-bending (kinking) motion, and (2) swiveling (twisting) motion[4,8] (Fig. 3). We have analyzed helix kink angles (i.e., hinge-bending) but will also consider swiveling motions. For both the Alm and Ala_{20}, simulations the kink angle was measured as a function of time. For Alm, the kink angle is approximately 30° at the start of the simulation. It fluctuates about this mean value, showing occasional excursions to significantly higher values, some of which last for approximately 250 ps [Fig. 4(A)]. Comparison of the kink angle distributions shows that the mean Alm kink angle is approximately 30° and the distribution is approximately normal (corresponding to an approximately quadratic effective potential function for kinking), although there is a noticeable tail at large kink angles. The corresponding distribution for Ala_{20} has a smaller standard deviation and an average of less than approximately 10°. Note that Ala_{20} is an unkinked helix and so its "kink angle" distribution reflects the effects of small deviations from helicity on the estimate of this angle. We note that Shen et al.[52] saw small deviations from helicity in a simulation of an Ala_{30} helix in a lipid bilayer.

The structural consequences of the fluctuations in the Alm helix kink angle are illustrated in Figure 5. Snapshots of the Alm structure taken every 250 ps from the simulation are superimposed using the 11 Cα atoms of the N-terminal segment of the molecule. From this it can be seen that the GxxP motif provides both hinge bending [Fig. 5(A)] and, to a lesser extent, twisting [Fig. 5(B)] motions. This is in agreement with previous studies of proline hinges in helices,[8,18] The snapshots confirm the helix kink angle analysis in suggesting both small and more major fluctuations about a mean of approximately 30°.

Analysis of the Alm motions using essential dynamics and DynDom revealed clear domain motions [Fig. 5(C)]. The first eigenvector describes a hinge-bending motion with 92% closure motion and a screw axis that is close to perpendicular to the line joining the centers of mass of the two domains (residues 1–10 and 11–20), with Gly11-Aib13 acting as mechanical hinges. The total angle of rotation of the domains around the screw axis is as much as 65°. The projections of the eigenvectors show that the first eigenvector has an autocorrelation time of the order of a nanosecond, so that this eigenvector is well defined in the 10-ns simulation. A projection of the first 2 or 3 eigenvectors in a plane or cubic grid shows that alamethicin moves within one minimum throughout the simulation. The second and third eigenvectors represent twisting motions with a much smaller amplitude.

Analysis of backbone torsion angles indicated that the structures shown in Figure 5A did not exhibit any backbone torsion angles that deviated significantly from the α-helical region of a Ramachandran plot, other than for residues at the helix termini. This suggests that Alm helix distortions resulted from the cumulative effect of relatively small deviations of torsion angles from the canonical α-helical values. However, analysis of percentage helicity vs. residue number revealed a drop from an average value of approximately 75% for "core" α-helical residues (e.g., residues 4 to 10) to approximately 55% for Gly11. Overall, these analyses suggest that the GxxP motif of Alm provides a dynamic hinge via transient disruption of intrahelical H-bonding. We note that nanosecond simulations of an Alm helix either in a box of methanol[51] or of octane (Tieleman et al., unpublished results) also exhibit fluctuations in helix kink angle, suggesting that an interfacial environment is not necessary for hinge-bending motion to occur.

TABLE I. Summary of Simulations

Simulation	Peptide length	Bilayer	Number of waters	Number of atoms	Duration (ns)
Ala20	20-mer	182 octanes	1,618	6,436	10
Alm	20-mer	182 octanes	1,618	6,478	10
KvS6/POPC	30-mer	127 POPCs	3,878	18,518	10
KvS6/octane	30-mer	702 octanes	4,781	20,239	10
hCLC1-S6	28-mer	182 octanes	1,789	7,062	5

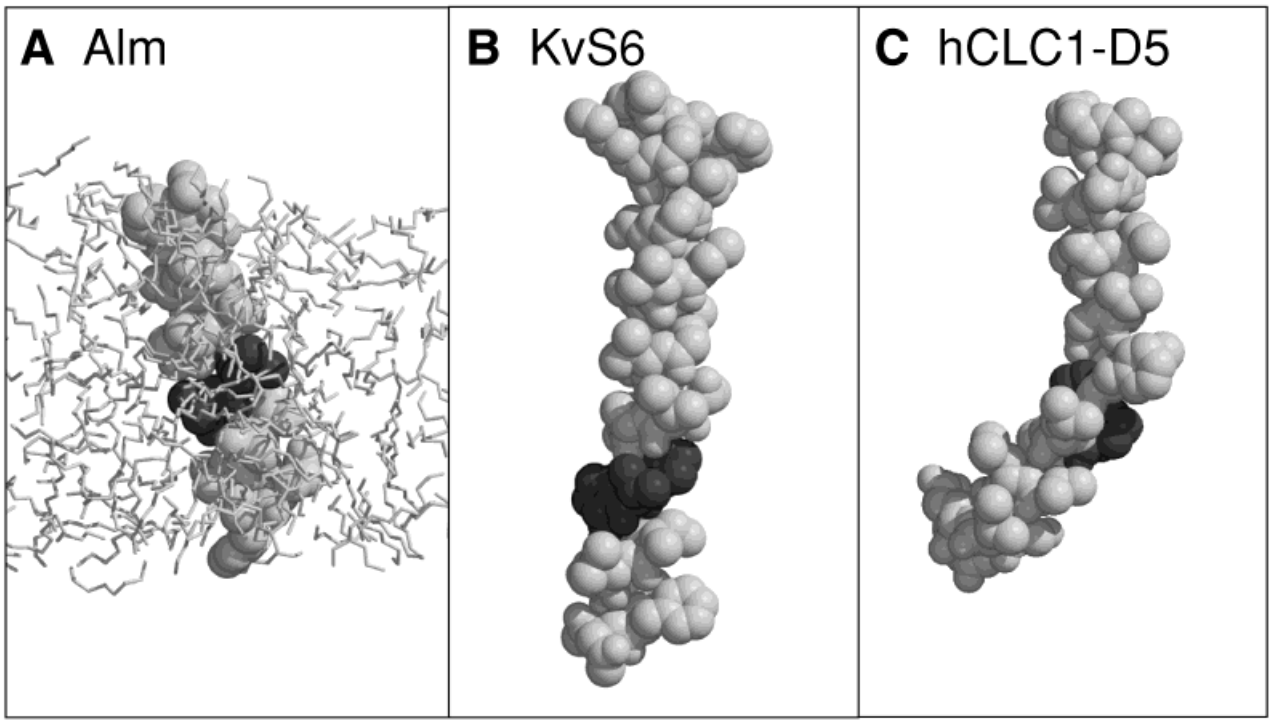

Fig. 2. Initial structures for the simulations: **A:** Alm helix in an octane slab. The central GxxP motif is shown in dark gray; **B:** Kv-S6 helix, with the PVP motif in dark gray; **C:** hCLC1-D5 helix, with the GxP motif in dark gray.

Kv-S6

It is of interest to extend our analysis to proline-induced hinges in TM helices from ion channel proteins. Perhaps the best-studied system is the S6 helix from voltage-gated potassium (Kv) channels (Fig. 1). The KvS6 helix contains a conserved sequence motif P-[V,I]-P, i.e., two prolines separated by a valine, or more rarely an isoleucine. Previous in vacuo simulations[15] and a short (1-ns) simulation in a lipid bilayer[23] suggested that the PVP motif of the Shaker KvS6 helix forms a kink in the helix. However, in the bilayer MD simulations only a single major fluctuation in the kink angle was seen, i.e., the simulation time was insufficient for proper sampling. Encouragingly, recent experimental studies on Kv channels using cysteine scanning mutagenesis and blocker protection studies[53] are consistent with a kink in S6. Thus, we have extended the simulation of KvS6 in a bilayer to 10 ns and also run a simulation of S6 in an octane slab (Table I). This provides an opportunity to better study the range of structures adopted by KvS6, and also yields a comparison of simulations in a lipid bilayer vs. simulations in an octane slab.

Helix kink angle trajectories are shown in Figure 6. In the KvS6/POPC trajectory, the helix kink angle seems to drift upwards for the first approximately 2 ns and then oscillates about 30°. In the KvS6/octane simulation, there is no obvious initial drift, and the oscillations are more rapid. The kink angle distributions are compared in Figure 7(A). Both systems show quite broad kink angle distributions. For KvS6/octane, the mode of the distribution is approximately 17°, whereas for KvS6/POPC it is approximately 30°. We have attempted to quantify the different time scales of the fluctuations in KvS6/POPC and KvS6/octane by evaluating the kink angle autocorrelation functions [ACFs; Fig. 7(B)]. From inspection of the ACFs, it is evident that the KvS6/octane fluctuations are on an approximately 100-ps time scale, whereas the time scale is at least 0.5 ns for the main kink angle fluctuations in KvS6/POPC. Thus, for a given simulation time, the octane slab simulation provides better sampling of helix hinge dynamics.

Comparison of the superimposed Cα traces for the simulations (Fig. 8) suggests that the overall nature of the

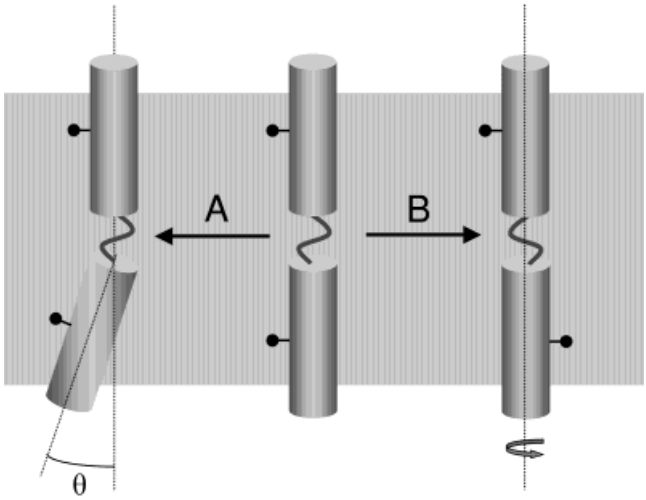

Fig. 3. Schematic digram of A kink and B swivel of a transmembrane helix about a central hinge.

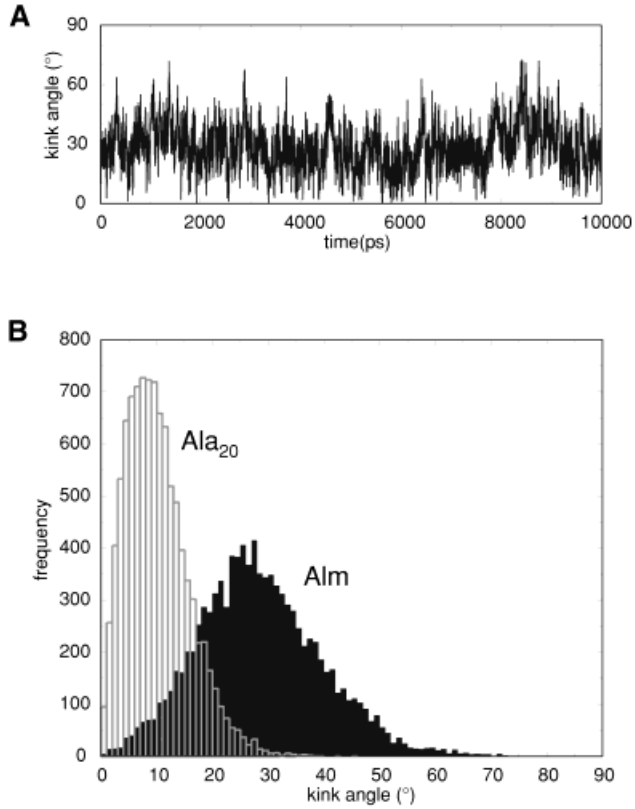

Fig. 4. Alm and Ala_{20} kink angles compared. **A:** Kink angle trajectory for the Alm simulation; **B:** Kink angle distributions for the Ala_{20} (gray, unfilled) and Alm (black, filled) simulations.

motion is similar in the two simulations (i.e., predominantly hinge bending with relatively little swivel). The magnitude of the changes is, indeed, somewhat greater in the lipid bilayer simulations. However, one must keep in mind the poorer sampling in lipid bilayer than in octane simulations.

Essential dynamics and DynDom analysis revealed that the first eigenvector of S6 in octane, with domains 3′–16′ and 17′–28′ describes a twisting motion between domains 2′–17′ and 18′–29′, i.e., twisting of domains defined by the PVP motif (residues 21′–23′) is not well defined in 10 ns. The second eigenvector shows some degree of hinge-bending motion between two domains, consisting of residues 2′–14′ and 15′–29′, with Gly14′–Thr-17′ acting as mechanical hinge, and 48% closure motion. The screw axis is at an angle of 48° with the line joining the centers of mass.

In POPC, the dynamics are much slower and the definition of the eigenvectors is incomplete. Taking residues 3′–27′ over the full 10 ns gives a picture of motion within 3 minima with long correlation times for the first eigenvector. The third eigenvector is broken in three domains, 3′–8′, 15′–19′, and 20′–25′, where the motion between the first two domains is twisting and between the middle and last domain is 49% closure. Thus, in both simulations there appear to be hinges in the vicinity of the glycine residue, and in the vicinity of (i.e., one turn before) the PVP motif.

Ramachandran plot analysis did not show any significant deviations of residue backbone torsion angles from the α-helical region (other than for residues at the helix termini). Thus, as with Alm, it would seem that helix motions are due to cumulative small backbone distortions. For both KvS6 simulations, the percentage helicity (averaged over the duration of the simulation) is significantly lower for residue 18′. This is one turn of the helix before the first proline of the PVP motif (and thus lies in the mechanical hinge region discussed above), indicating that hinge dynamics are associated with a break in intrahelical H-bonding induced by that proline. The greater kink angle of KvS6/POPC was associated with a bigger drop in helicity than for KvS6/octane.

hCLC1-D5

Having established that a proline-containing motif in the center of a TM helix may be associated with formation of a dynamic hinge, the SWISSPROT sequence database was searched (using ScanProsite, http://www.expasy.ch/tools/scnpsit2.html) for the presence of either a P-[V,I]-P or of a (GxP or GxxP) motif within a hydrophobic region of sufficient length to span a bilayer. Only those "hits" for which the motif was conserved between all/most homologues were considered further. For the P-[V,I]-P motif, the only convincingly conserved hit was for Kv channels. However, the GxP or GxxP search yielded a significant hit for a further family of voltage-gated ion channels, namely the voltage-gated chloride channels (CLCs).[54,55] (CLCs are important in, e.g., regulating muscle chloride conductance, and their malfunction can lead to myotonia[56]). A GxP motif is conserved in the sequence of helix D5 of CLCs (as may be seen from a sequence alignment of D5 from human CLCs; Fig. 1). Although the structure of CLC is not known, there is evidence to implicate D5 in slow gating by this channel.[57] It is, thus, striking that it contains this highly conserved motif. As can be seen from Figure 2, an initial model of hCLC1-D5, generated by restrained MD in vacuo,

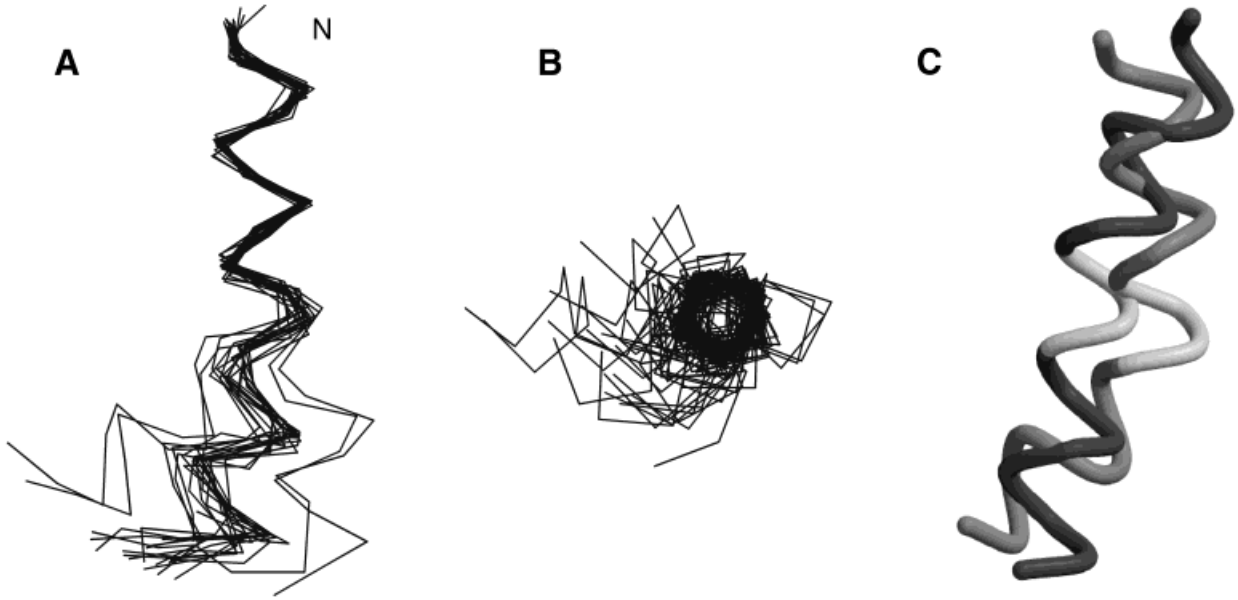

Fig. 5. Snapshots from the Alm simulation, showing superimposed Cα traces (saved every 250 ps for 10 ns), with the N-terminal half (residues 1–11) of each helix superimposed. **A:** View perpendicular to the N-terminal helix axis. **B:** View down the N-terminal helix axis. **C:** Two extreme conformations of Alm, identified by essential dynamics and DynDom analysis, indicating a hinge bending motion of two domains (residues 1–10 and 11–20), with Gly11-Aib13 (light gray) acting as mechanical hinge.

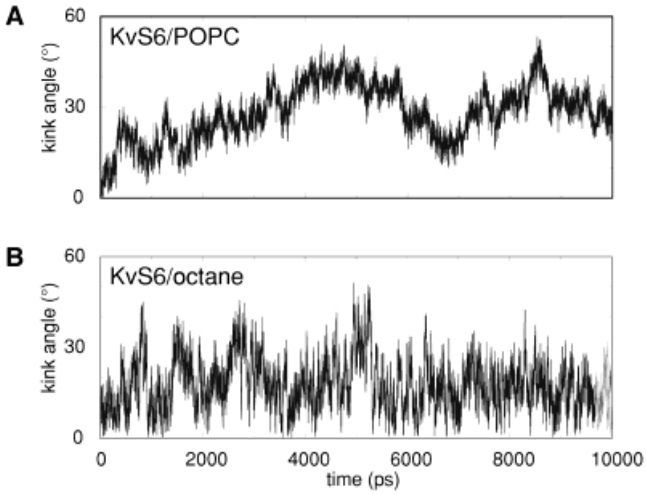

Fig. 6. Kink angle trajectories for the (**A**) KvS6/POPC and (**B**) KvS6/octane simulations.

had a pronounced kink in the vicinity of the GxP motif. This model was used as the starting structure for a 5-ns simulation of D5 in an octane slab (Table I).

The kink angle trajectory of D5 [Fig. 9(B)] shows large fluctuations (from approximately 25° to greater than 60°) to occur on a time scale of several ns. In this case, the kink angle fluctuations could be seen to be highly correlated with the backbone torsion angle Ψ of the G16′ residue [Fig. 9(A)]. Thus, the large kink angle of D5 in the first ns or so of the simulation is associated with this glycine leaving the α-helical region of the Ramachandran plot. The complexities of the motion about the GxP hinge in D5 are reflected in the bimodal distribution of kink angles. This simulation is of interest in that it suggests that hinge dynamics take >1 ns even in octane.

In the D5 simulation, the projection of the first 3 eigenvectors reveals long correlation times, of the order of half the simulation length. The first eigenvector is dominated by jumps between different minima, and represents mostly a twisting motion of residues 2′–16′ with respect to residues 17′–25′. The second eigenvector describes hinge bending with two domains, from 3′–16′ and 17′–25′, with Phe15′ and Gly16′ (i.e., the glycine of the GxP motif) acting as a mechanical hinge. The motion is 71% closure, and the domains show a rotation of 51° around a screw axis that is at an angle of 58° to the line between the centers of mass of the two domains. The third eigenvector also is characterized by a twisting motion of residues 3′–18′ with respect to residues 19′–25′, around an axis almost parallel to the line joining the centers of mass of these domains.

The superimposed snapshots of the D5 helix confirm the complexities of the motion (Fig. 10). It appears to contain both a hinge-bending and swiveling component. Other than in the vicinity of the GxP motif (and at the termini) the α-helical conformation appears to be preserved. Analysis of average percentage helicity vs. residue number (data not shown) shows a drop below 40% for G16′ (i.e., the G of GxP). Corresponding drops in helicity are not seen for the five other glycine residues in the hCLC1-D5 sequence. Overall, the various analyses suggest that the combination of a glycine and proline forms a dynamic hinge in D5.

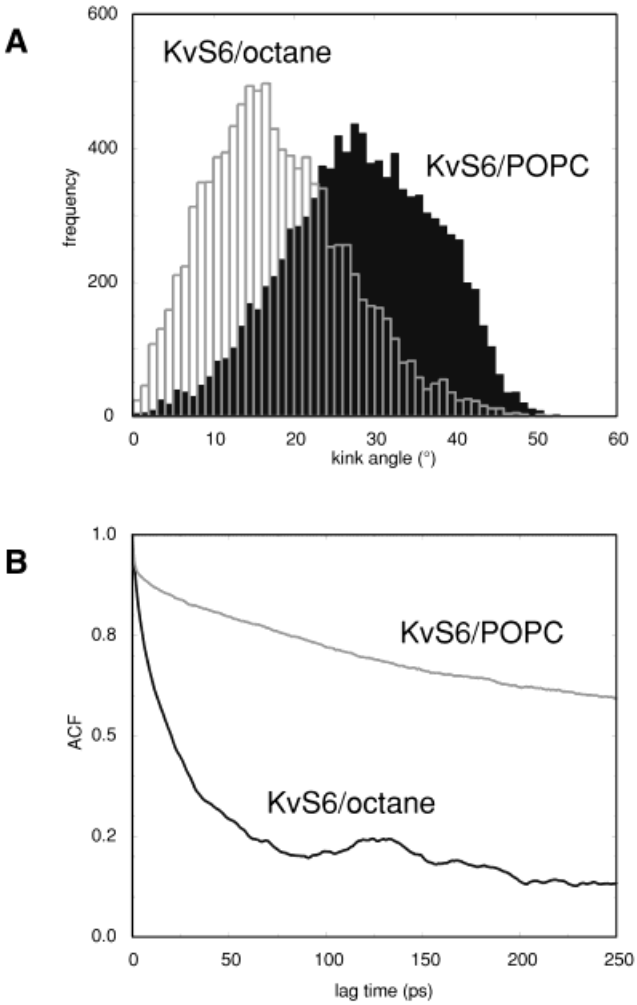

Fig. 7. KvS6-kink angle distributions and autocorrelation functions (ACFs). **A:** Kink angle distributions for the KvS6/POPC and KvS6/octane simulations; **B:** Kink angle ACFs derived from the same trajectories. Note that the ACFs were calculated for the period 2 to 10 ns for each simulation in order to exclude the effect of any initial "drift" in kink angle.

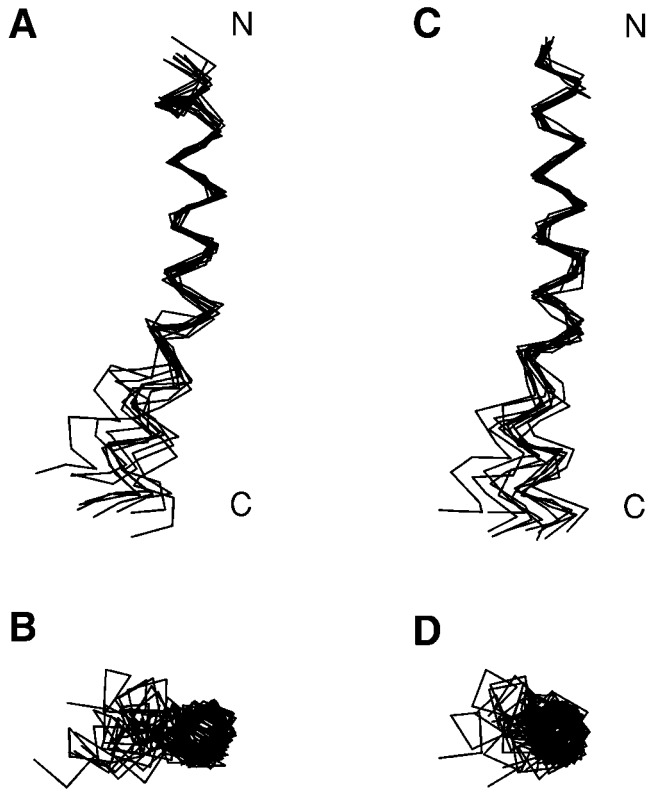

Fig. 8. Snapshots from the KvS6 simulations, shown as superimposed Cα traces saved every 1 ns for 10 ns. The superimposition was of Cα atoms N-terminal to the PVP hinge. The view in **B,D** is perpendicular to that in **A,C**, i.e., down the S6 helix with the N-terminus towards the viewer. A,B: KvS6/POPC; C,D: KvS6/octane.

DISCUSSION

Critical Review of Simulation Methods Employed in this Study

In this review, we present evidence that proline-induced kinks in transmembrane α-helices can act as dynamic hinges when such helices are embedded in a bilayer or a bilayer-mimetic environment. However, even in the rather more fluid environment provided by an octane slab, motion about such hinges may occur on a time scale of up to a nanosecond. This explains why previous, somewhat shorter, simulations of, e.g., KvS6, provided poor sampling of such motions. Indeed, even the current simulations may require extension (possibly by an order of magnitude[34]) to provide good sampling. An alternative, already explored for small water soluble proteins (e.g.,[58]), is to perform multiple shorter runs. Preliminary studies (Bright and Sansom, unpublished results) suggest that the latter may be appropriate for further studies of S6.

One should consider the question of the relevance of simulation studies on single TM helices to an understanding of possible mechanisms of channel gating. It is evident that helix packing interactions within a multi-TM helix protein may modulate the hinge-bending and twisting motions seen in the current study. However, it is also evident that the long time scale dynamics (i.e., gating) of a channel protein should embody the flexibility of the components of that protein. The comparison of KvS6 hinge-bending in an octane slab vs. a lipid bilayer suggests that while the fundamental motions of the helix might be similar, their time scale is dominated by their environment. Thus, within a channel protein one might expect even slower hinge-bending motions of S6, possibly on a time scale associated with channel gating. Perhaps by quantifying the relative viscosities of octane, POPC, and protein environments, it might be possible to estimate the likely frequency of KvS6 hinge-bending within a channel molecule.

However, we should not assume that the differences between the POPC and octane simulations are simply differences in sampling. Clearly, a POPC bilayer provides a rather more complex interfacial environment than does an octane slab. In particular, it is possible that hinge-bending motions might be coupled to the (slow) interfacial fluctuations of a bilayer.[59] To explore this aspect further

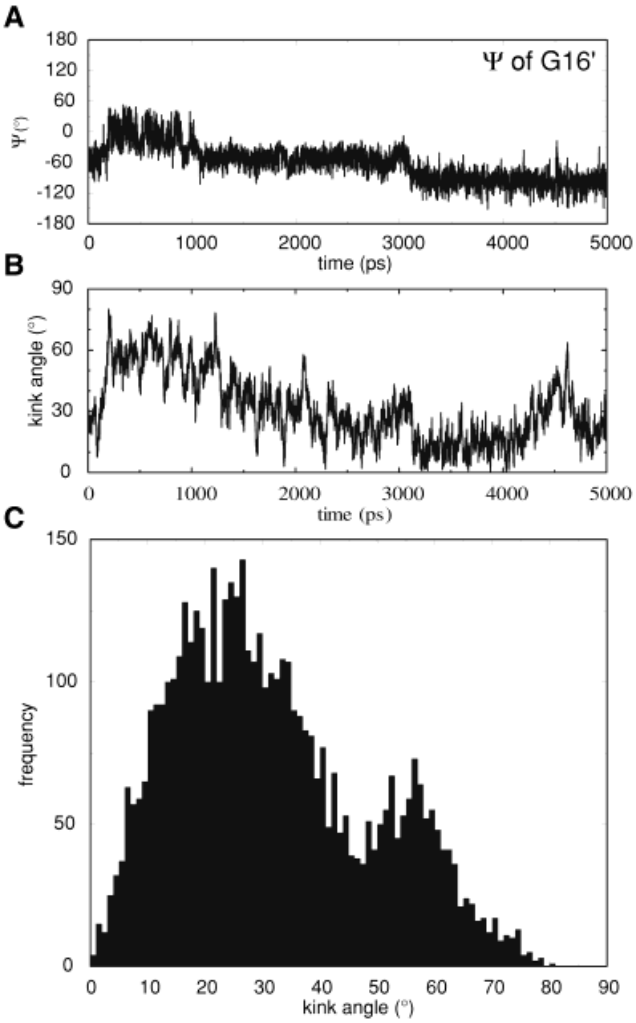

Fig. 9. Analysis of the HCLC1-D5 simulation. **A:** Backbone torsion angle (Ψ of G16′). **B:** Kink angle trajectory and (**C**) kink angle distribution for hCLC1-D5.

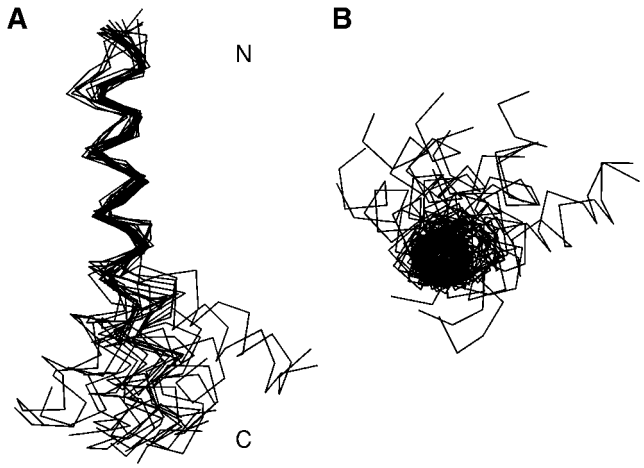

Fig. 10. hCLC1-D5-superimposed Cα traces saved every 250 ps for 5 ns. The superimposition is of the Cα atoms N-terminal to the GxP hinge region. The view in **B** is perpendicular to that in **A**, i.e., down the D5 helix with the N-terminus toward the viewer.

may require multiple extended simulations in different sized bilayers.

Possible Biological Relevance

What is the possible biological relevance of these simulation results? One should be cautious in over-interpreting such studies, especially as there is not yet a three-dimensional structure available for an intact voltage-gated ion channel. However, by combining the simulation results presented above with various strands of (indirect) evidence it is possible to arrive at a plausible model for the role(s) of proline-induced hinges in channel gating, at least for Kv channels.

Firstly, it is important to re-iterate that intra-helical prolines are quite common in transmembrane α-helices, even though proline is sometimes thought of as a "helix-breaking" residue.[60] The relatively high frequency of prolines in predicted TM helices was noted by Deber and colleagues,[5] and this analysis has recently been extended.[9] It is also possible to analyze the frequency of occurrence of intra-helical prolines in membrane proteins of known three-dimensional structure. Thus, comparison of the distribution of proline residues along TM α-helices with the distribution of a typical hydrophobic sidechain (e.g., Val)[61] shows that although proline occurs more frequently at either end of the helix, there is a significant occurrence of proline within the transbilayer region.

Having established that proline residues are widespread in TM α-helices, what about their effect on TM helix conformation? At an anecdotal level, several kinked TM α-helices are seen in X-ray structures, such as: (1) TM helix G from ubiquinol cytochrome c oxidoreductase (1bcc); (2) two TM helices of the CaATPase (1eul); and (3) three TM helices (M1, M6, and M7) of rhodopsin (1f88). Given the growing database of TM helices, a more systematic survey might be worthwhile.

In addition to structural data, there are also functional studies of voltage-gated ion channels that implicate proline residues in possible gating mechanisms. For Alm, the data are perhaps a little difficult to interpret,[62,62] but they do suggest that changes to the GxxP motif alter the dynamics of gating of Alm channels.[64] Substitutions for the proline in the related peptide melittin also perturb its interactions with membranes.[14] Recent studies[65] on the anti-microbial peptide buforin2 indicate that loss of proline from a GxxxP motif removes the ability of this peptide to cross cell membranes. Proline-induced kinks seem to be important in the biological activities of other antimicrobial peptides, such as maculatin[66] and gaegurin.[67] Thus, it would appear that a proline-induced hinge may play a functional role in the insertion of antimicrobial peptides into membranes. For Kv channels, Swartz and colleagues[12] have shown that mutations of the PVP motif in S6 result in significant alterations to channel gating. Structure/function relations in CLC channels have been explored in less detail (as only a low-resolution projection structure is at present available[68]), but there is some evidence that a mutation in D5 can alter the slow (voltage-dependent) gating of the channel.[57]

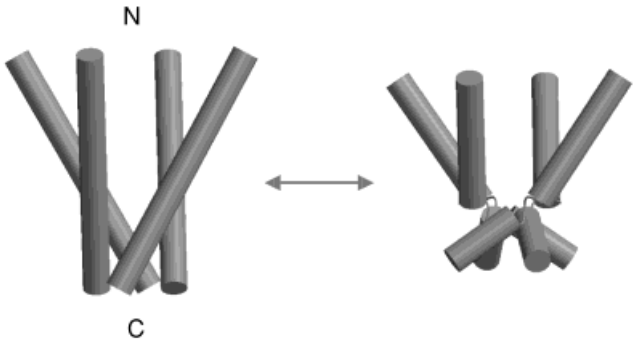

Fig. 11. The inner helix bundle of a Kv channel is believed to be formed by four S6 helices. A possible model of channel gating might invoke transitions between a model based on the X-ray structure of the bacterial channel KcsA, built from undistorted S6 helices (**left**) and a similar model, but containing kinked S6 helices taken from the KvS6/POPC simulation (**right**).

Probably our best model of how a proline-induced kink may be involved in channel-gating can be constructed for Kv. Yellen and colleagues[53] have presented data consistent with a "kinked S6" model. Spin label studies[3,69] on the (voltage-independent) gating mechanism of the simpler but structurally homologous bacterial channel KcsA[1] suggest repacking of the M2 helices (the bacterial homologue of S6, which, however, does not include a PVP motif) underlies channel gating. Small changes in the conformation of the M2 helices, possibly related to channel gating, have been seen in simulations of KcsA[70] (see also, Shrivastava and Sansom, unpublished results). Thus, it is possible (see Fig. 11) that the "opening" of the S6 bundle may involve changes in helix conformation (e.g., unkinked to kinked or vice versa) in addition to a change in helix packing. Clearly direct structural studies are needed to prove this, but this proposal seems to be sufficiently plausible to warrant further investigation. In passing, we note that a model involving repacking of kinked helices has been invoked to explain the mechanism of gating of the nicotinic acetylcholine receptor.[71]

ACKNOWLEDGMENTS

Our thanks to all of our colleagues, especially Dr. Harel Weinstein (Mount Sinai Medical School) and Dr. Oliver Smart (Birmingham University) for helpful discussions. Additional computer time was provided by the Oxford Supercomputing Centre. D.P.T. was supported by an EMBO fellowship, and is now an AHFMR Scholar. M.B.U. is a MRC research student.

REFERENCES

1. Doyle DA, Cabral JM, Pfuetzner RA, Kuo A, Gulbis JM, Cohen SL, Cahit BT, MacKinnon R. The structure of the potassium channel: molecular basis of K+ conduction and selectivity. Science 1998;280: 69–77.
2. Chang G, Spencer RH, Lee AT, Barclay MT, Rees DC. Structure of the MscL homolog from Mycobacterium tuberculosis: a gated mechanosensitive ion channel. Science 1998;282:2220–2226.
3. Perozo E, Cortes DM, Cuello LG. Structural rearrangements underlying K^+-channel activation gating. Science 1999;285:73–78.
4. Sansom MSP, Weinstein H. Hinges, swivels & switches: the role of prolines in signalling via transmembrane α-helices. Trends Pharm Sci 2000;21:445–451.
5. Brandl CJ, Deber CM. Hypothesis about the function of membrane-buried proline residues in transport proteins. Proc Natl Acad Sci USA 1986;83:917–921.
6. Barlow DJ, Thornton JM. Helix geometry in proteins. J Mol Biol 1988;201:601–619.
7. von Heijne G. Proline kinks in transmembrane α-helices. J Mol Biol 1991;218:499–503.
8. Sankararamakrishnan R, Vishveshwara S. Geometry of proline-containing alpha-helices in proteins. Int J Pept Prot Res 1992;39: 356–363.
9. Senes A, Gerstein M, Engelman DM. Statistical analysis of amino acid patterns in transmembrane helices: The GxxxG motif occurs frequently and in association with beta-branched residues at neighboring positions. J Mol Biol 2000;296:921–936.
10. Woolfson DN, Mortishire-Smith RJ, Williams DH. Conserved positioning of proline residues in membrane-spanning helices of ion-channel proteins. Biochem Biophys Res Commun 1991;175: 733–737.
11. Sansom MSP. Proline residues in transmembrane helices of channel and transport proteins: a molecular modelling study. Prot Eng 1992;5:53–60.
12. Hackos DH, Swartz KJ. Mutations of a conserved proline in the inner helix of the pore domain of the Shaker K^+ channel with altered gating properties. Biophys J 2000;78:398A.
13. Sansom MSP. Structure and function of channel-forming peptaibols. Q Rev Biophys 1993;26:365–421.
14. Dempsey CE, Bazzo R, Harvey TS, Syperek I, Boheim G, Campbell ID. Contribution of proline-14 to the structure and actions of melittin. FEBS Lett 1991;281:240–244.
15. Kerr ID, Son HS, Sankararamakrishnan R, Sansom MSP. Molecular dynamics simulations of isolated transmembrane helices of potassium channels. Biopolymers 1996;39:503–515.
16. Polinsky A, Goodman M, Williams KA, Deber CM. Minimum energy conformations of proline-containing helices. Biopolymers 1992;32:399–406.
17. Yun RH, Anderson A, Hermans J. Proline in α-helix: stability and conformation studied by dynamics simulation. Proteins 1992;10: 219–228.
18. Sankararamakrishnan R, Vishveshwara S. Characterisation of proline-containing α-helix (helix F model of bacteriorhodopsin) by molecular dynamics studies. Proteins 1993;15:26–41.
19. Vishveshwara SS, Vishveshwara S. Effect of constraints by threonine on proline containing α-helix: a molecular dynamics approach. Biophys Chem 1993;46:77–89.
20. Iyer LK, Vishveshwara S. Threonine mutations in proline helix II of bacteriorhodopsin: a molecular dynamics study. J Mol Struct (Theochem) 1996;361:269–281.
21. Tieleman DP, Marrink SJ, Berendsen HJC. A computer perspective of membranes: molecular dynamics studies of lipid bilayer systems. Biochim Biophys Acta 1997;1331:235–270.
22. Forrest LR, Sansom MSP. Membrane simulations: bigger and better? Curr Opin Struct Biol 2000;10:174–181.
23. Shrivastava IH, Capener C, Forrest LR, Sansom MSP. Structure and dynamics of K+ channel pore-lining helices: a comparative simulation study. Biophys J 2000;78:79–92.
24. Kerr ID, Sankararamakrishnan R, Smart OS, Sansom MSP. Parallel helix bundles and ion channels: molecular modelling via simulated annealing and restrained molecular dynamics. Biophys J 1994;67:1501–1515.
25. von Heijne G. Membrane protein structure prediction. Hydrophobicity analysis and the positive inside rule. J Mol Biol 1992;225: 487–494.
26. Persson B, Argos P. Prediction of transmembrane segments utilising multiple sequence alignments. J Mol Biol 1994;237:182–192.
27. Persson B, Argos P. Prediction of membrane protein topology utilizing multiple sequence alignments. J Prot Chem 1997;16:453–457.
28. Cserzo M, Wallin E, Simon I, von Heijne G, Elofsson A. Prediction of transmembrane alpha-helices in prokaryotic membrane proteins: the dense alignment surface method. Prot Eng 1997;10:673–676.
29. Rost B, Casadio R, Fariselli P, Sander C. Prediction of helical transmembrane segments at 95% accuracy. Prot Sci 1995;4:521–533.

30. Rost B, Fariselli P, Casadio R. Topology prediction for helical transmembrane proteins at 86% accuracy. Prot Sci 1996;5:1704–1718.
31. Jones DT, Taylor WR, Thornton JM. A model recognition approach to the prediction of all-helical membrane protein structure and topology. Biochem 1994;33:3038–3049.
32. Sonnhammer ELL, von Heijne G, Krogh A. A hidden Markov model for predicting transmembrane helices in protein sequences. In: Glasgow J, Major TLF, Lathrop R, Sankoff D, Sensen C, editors. Proc of Sixth Int Conf on Intelligent Systems for Molecular Biology. AAAI Press; 1988. p 175–182.
33. Hofmann K, Stoffel W. TMBASE: a database of membrane spanning protein segments. Biol Chem Hoppe-Seyler 1993;374:166.
34. Tieleman DP, Berendsen HJC, Sansom MSP. Voltage-dependent insertion of alamethicin at phospholipid/water and octane/water interfaces. Biophys J 2000;80:331–346.
35. Berendsen HJC, van der Spoel D, van Drunen R. GROMACS: A message-passing parallel molecular dynamics implementation. Comp Phys Comm 1995;95:43–56.
36. Hermans J, Berendsen HJC, van Gunsteren WF, Postma JPM. A consistent empirical potential for water-protein interactions. Biopolymers 1984;23:1513–1518.
37. van Gunsteren WF, Kruger P, Billeter SR, Mark AE, Eising AA, Scott WRP, Huneberger PH, Tironi IG. Biomolecular simulation: the GROMOS96 manual and user guide. Zurich: Biomos & Hochschulverlag AG an der ETH; 1996.
38. Feenstra KA, Hess B, Berendsen HJC. Improving efficiency of large time-scale molecular dynamics simulations of hydrogen-rich systems. J Comp Chem 1999;20:786–798.
39. Hess B, Bekker H, Berendsen HJC, Fraaije JGEM. LINCS: A linear constraint solver for molecular simulations. J Comp Chem 1997;18:1463–1472.
40. Berendsen HJC, Postma JPM, van Gunsteren WF, DiNola A, Haak JR. Molecular dynamics with coupling to an external bath. J Chem Phys 1984;81:3684–3690.
41. Kraulis PJ. MOLSCRIPT: a program to produce both detailed and schematic plots of protein structures. J Appl Cryst 1991;24:946–950.
42. Merritt EA, Bacon DJ. Raster3D: photorealistic molecular graphics. Methods Enzymol 1997;277:505–524.
43. Amadei A, Linssen ABM, Berendsen HJC. Essential dynamics of proteins. Proteins 1993;17:412–425.
44. Berendsen HJC, Hayward S. Collective protein dynamics in relation to function. Curr Opin Struct Biol 2000;10:165–169.
45. Hayward S, Berendsen HJC. Systematic analysis of domain motions in proteins from conformational change: new results on citrate synthase and T4 lysozyme. Proteins 1998;30:144–154.
46. Woolley GA, Wallace BA. Model ion channels: gramicidin and alamethicin. J Membr Biol 1992;129:109–136.
47. Cafiso DS. Alamethicin: a peptide model for voltage gating and protein membrane interactions. Ann Rev Biophys Biomol Struct 1994;23:141–165.
48. Fox RO, Richards FM. A voltage-gated ion channel model inferred from the crystal structure of alamethicin at 1.5 Å resolution. Nature 1982;300:325–330.
49. Esposito G, Carver JA, Boyd J, Campbell ID. High resolution ^{1}H NMR study of the solution structure of alamethicin. Biochemistry 1987;26:1043–1050.
50. Gibbs N, Sessions RB, Williams PB, Dempsey CE. Helix bending in alamethicin: molecular dynamics simulations and amide hydrogen exchange in methanol. Biophys J 1997;72:2490–2495.
51. Tieleman DP, Sansom MSP, Berendsen HJC. Alamethicin helices in a bilayer and in solution: molecular dynamics simulations. Biophys J 1999;76:40–49.
52. Shen L, Bassolino D, Stouch T. Transmembrane helix structure, dynamics, and interactions: multi-nanosecond molecular dynamics simulations. Biophys J 1997;73:3–20.
53. Camino DD, Holmgren M, Liu Y, Yellen G. Blocker protection in the pore of a voltage-gated K^+ channel and its structural implications. Nature 2000;403:321–325.
54. Jentsch TJ, Friedrich T, Schriever A, Yamada H. The CLC chloride channel family. Pflug Arch Eur J Physiol 1999;437:783–795.
55. Maduke M, Miller C, Mindell JA. A decade of CLC chloride channels: structure, mechanism, and many unsettled questions. Annu Rev Biophys Biomol Struct 2000;29:411–438.
56. Ashcroft FM. Ion channels and disease. San Diego: Academic Press, 2000.
57. Lin YW, Lin CW, Chen TY. Elimination of the slow gating of ClC-0 chloride channel by a point mutation. J Gen Physiol 1999;114:1–12.
58. Caves LSD, Evanseck JD, Karplus M. Locally accessible conformations of proteins: multiple molecular dynamics simulations of crambin. Prot Sci 1998;7:649–666.
59. Lindahl E, Edholm O. Mesoscopic undulations and thickness fluctuations in lipid bilayers from molecular dynamics simulations. Biophys J 2000;79:426–433.
60. Richardson JS, Richardson DC. Principles and patterns of protein conformation. In: Fasman GD, editor. Prediction of protein structure and the principles of protein conformation. New York: Plenum Press; 1989. p 1–98.
61. Ulmschneider MB, Sansom MSP. Amino acid distributions in integral membrane protein structures. Biochim Biophys Acta 2001;1512:1–14.
62. Duclohier H, Molle G, Dugast J-Y, Spach G. Prolines are not essential residues in the "barrel-stave" model for ion channels induced by alamethicin analogues. Biophys J 1992;63:868–873.
63. Jacob J, Duclohier H, Cafiso DS. The role of proline and glycine in determining backbone flexibility of a channel-forming peptide. Biophys J 1999;76:1367–1376.
64. Kaduk C, Dathe M M. B. Functional modifications of alamethicin ion channels by substitution of glutamine 7, glycine 11 and proline 14. Biochim Biophys Acta 1998;1373:137–146.
65. Park CB, Yi KS, Matsuzaki K, Kim MS, Kim SC. Structure-activity analysis of buforin II, a histone H2A-derived antimicrobial peptide: The proline hinge is responsible for the cell-penetrating ability of buforin II. Proc Natl Acad Sci USA 2000;97:8245–8250.
66. Chia BCS, Carver JA, Mulhern TD, J.H. B. Maculatin 1.1, an anti-microbial peptide from the Australian tree frog, *Litoria genimaculata*: solution structure and biological activity. Eur J Biochem 2000;267:1894–1908.
67. Suh JY, Lee YT, Park CB, Lee KH, Kim SC, Choi BS. Structural and functional implications of a proline residue in the antimicrobial peptide gaegurin. Eur J Biochem 1999;266:665–674.
68. Mindell JA, Maduke M, Miller C, Grigorieff N. Projection structure of a CIC-type chloride channel at 6.5 angstrom resolution. Nature 2001;409:219–223.
69. Perozo E, Cortes DM, Cuello LG. Three-dimensional architecture and gating mechanism of a K+ channel studied by EPR spectroscopy. Nature Struct Biol 1998;5:459–469.
70. Shrivastava IH, Sansom MSP. Simulations of ion permeation through a potassium channel: molecular dynamics of KcsA in a phospholipid bilayer. Biophys J 2000;78:557–570.
71. Unwin N. Acetylcholine receptor channel imaged in the open state. Nature 1995;373:37–43.